



## STRENGTH AND STIFFNESS OF REINFORCED CONCRETE BEAM-COLUMN JOINTS WITH WELDED JOINTS FOR REINFORCING BARS OF BEAM AND STEEL PLATES

Y.HOSOKAWA, Y.SAKUTA, Y.HIROTA

Industrial Project Driving Office, Technology Division, Maeda Corporation,  
2-10-26,Fujimi, Chiyodaku, Tokyo, 102, Japan

S.KATO

Structural Engineering Section, Architectural Design Div., Maeda Corporation,  
2-10-26,Fujimi, Chiyodaku, Tokyo, 102, Japan

Y.MATSUZAKI, I.HASHIMOTO

Dept. of Architecture, Faculty of Eng., Science Univ. of Tokyo  
1-3, Kagurazaka, shinjiku, Tokyo, 162, Japan

### ABSTRACT

The paper proposes a new industrialized construction method for steel frame building structures. Developed to reduce labor requirements at construction sites and shorten construction periods, this new construction method, one based on reinforced concrete structure design concepts, is a mixed structural system whose assembly method incorporates the steel frame construction approach. The framework is made by forming HTB (High Tensile Bolt) joints to link thin reinforced concrete precast (PCa) beams with concrete filled steel tubes, then pouring the column and floor concrete to integrate the beams and tubes with the columns and floors. The connections characteristic of this type of framework are formed by steel frame flanges welded to the ends of the main reinforcement of the end connections of the PCa beams, and at the columns, stiffener rings used as beam flange connections welded to the steel pipes. The yield location during an earthquake is assumed to be the toe of the welded anchor of the beam's main reinforcement bars. This paper reports on the results of model testing of the structural capacity of these beam-column joints performed to contribute to the popularization of the method. The study confirmed that the strength and deformation capacity of these column-beam joints provide earthquake resistance equal to or greater than that of existing reinforced concrete structures.

### KEYWORDS

Mixed structural system, precast concrete, concrete filled tube column, plastic hinge, yield strength, ultimate strength, beam-column joint, welded joints.

### INTRODUCTION

Because beam-column joints in ordinary placed on-site reinforced concrete structures are formed by anchoring the reinforcing bars inside the columns, it is often the case that the work is complex, efficiency declines, and concrete placing is difficult wherever there are large quantities of reinforcement bars inside the columns or the beams. And the work is difficult because in order to also provide structural adhesive strength, the reinforcing steel bars are bent and anchored inside the columns.

This paper proposes a rationalized structural system developed by rationalizing joint execution so that it is possible to simultaneously place floor concrete and so on at many stories as in the case of the steel frame structure; its construction method is shown in Fig. 1.

Because this is a new structural system in which concrete filled tube columns are directly bolted to the PCa beams, few studies of its properties have been performed and little published information on this topic is available. Consequently, this experimental study of the strength of the joints between the steel reinforcement bars and the flange plates, the strength of the beam-column joints, and the hypothetical yield hinge positions was performed, confirming the earthquake resistance of the structural system, and providing research results for use in future studies of structural systems of this kind.

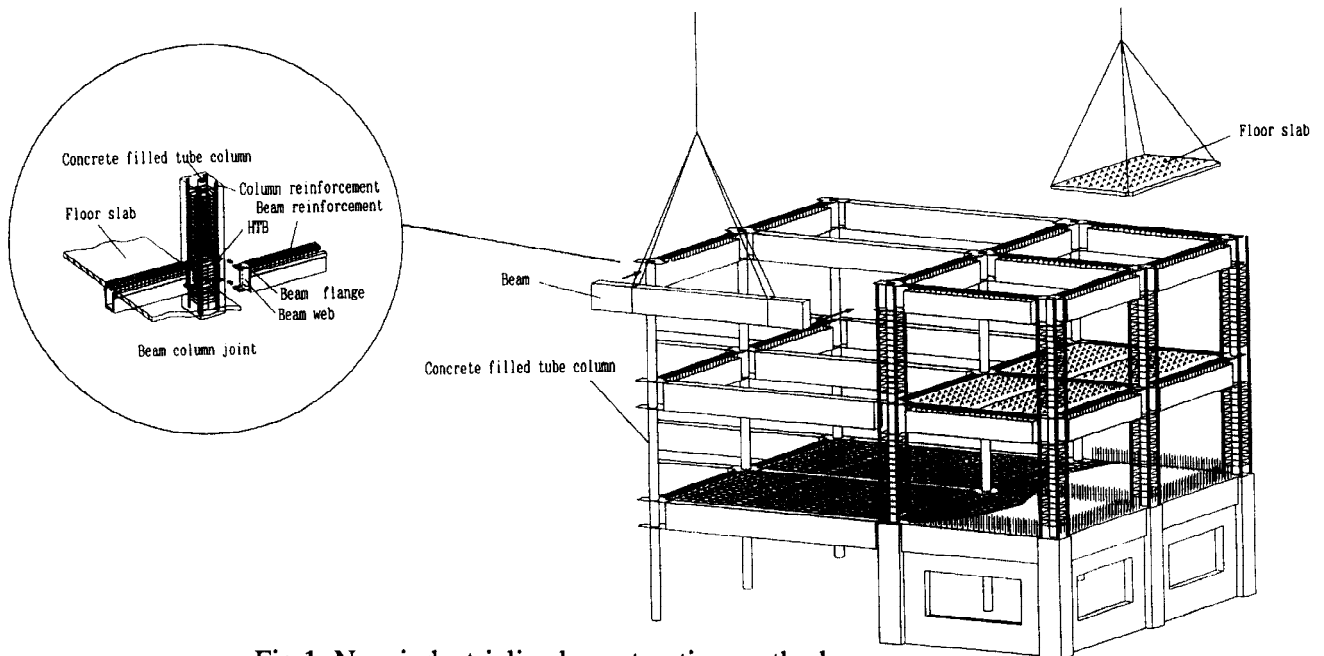


Fig.1 New industrialized construction methods

## TEST AND RESULT OF BEAM-COLUMN JOINTS

**Test specimens** Figure 2 shows the shape and dimensions of the test specimens, an outline of the beam and column cross sections, and the reinforcement and strain gauge locations. Cruciform type for inside columns and column joints include a total of 8 specimens: 6 specimens of this new structural system and 2 specimens of conventional reinforced concrete structures.

Two T-shaped specimens for outside columns brought the total number of test specimens to ten. The column cross section,  $B \times D = 50 \times 50\text{cm}$ , the beam cross section,  $b \times D = 30 \times 53\text{cm}$ , the story height 240cm, the span set at 500cm, and the scale was 1/1.7. Table 1 presents a specimen table and the forecast failure modes. The materials used and their mechanical properties are shown in Table 2. The basic design strength of the concrete  $F_c 240\text{kg/cm}^2$ .

Table 1 Characteristics of specimens

Test specimen		NEW STRUCTURAL SYSTEM (MIMNA-TYPE)								RC type	
		No.1 JSCB1	No.2 JDCB1	No.3 JDCP1	No.4 JDCP2	No.5 JDTP1	No.6 JDTP2	No.7 J-CP3-1	No.8 J-CP3-2	No.9 RC-B	No.10 RC-J
Col.	Reinforcing bar	12-D16	12-D19	12-D22	12-D25	12-D19	12-D22	12-D25	12-D25	12-D19	14-D25
	Hoop Tube column	2-U6.4@100 165.2 $\phi \times 4.5$	2-U6.4@60 165.2 $\phi \times 4.5$	4-U6.4@55 165.2 $\phi \times 4.5$	4-U6.4@35 165.2 $\phi \times 4.5$	2-U6.4@60 165.2 $\phi \times 4.5$	4-U6.4@55 165.2 $\phi \times 4.5$	4-U6.4@30 165.2 $\phi \times 7.1$	4-U6.4@30 216.3 $\phi \times 5.8$	2-U6.4@50 none	4-U6.4@30 none
Beam	Reinforcing bar	3-D19	6-D19	6-D22	4-D22,2-D25	6-D19	4-D22,2-D25	4-D25,2-D29	4-D25,2-D29	7-D19	6-D25
	Stirrup	2-U6.4@100	2-U6.4@100	4-U6.4@80	4-U6.4@60	2-U6.4@100	4-U6.4@60	4-U6.4@60	4-U6.4@60	2-U6.4@100	4-U6.4@100
	Flange	PL-9	PL-19	PL-25	PL-28	PL-19	PL-28	PL-28	PL-28	none	none
	Web	PL-4.5	PL-4.5	PL-6	PL-9	PL-4.5	PL-9	PL-9	PL-9	none	none
Joint	Hoop	2-D6@60	2-D6@60	2-D6@60	2-D6@60	2-D6@60	2-D6@60	2-D6@60	2-D6@60	2-D6@60	2-D6@60
	Stiffener ring	PL-9	2PL-12	2PL-16	2PL-16	2PL-12	2PL-16	PL-28	PL-28	none	none
	Web	PL-4.5	PL-4.5	PL-6	PL-9	PL-4.5	PL-9	PL-9	PL-9	none	none
Outline of specimen		Interior	Interior	Interior	Interior	Exterior	Exterior	Interior	Interior	Interior	Interior
Axial load (kgf/cm <sup>2</sup> )		0.2F <sub>c</sub>	0.2F <sub>c</sub>	0.2F <sub>c</sub>	0.2F <sub>c</sub>	0.1F <sub>c</sub>	0.1F <sub>c</sub>	0.2F <sub>c</sub>	0.2F <sub>c</sub>	0.2F <sub>c</sub>	0.2F <sub>c</sub>
Design failure mode		B	B	B-J	J	B	J	J	J	B	J

B : Beam yielding type , B-J : Beam yield before joint fail in shear , J : joint shear failure

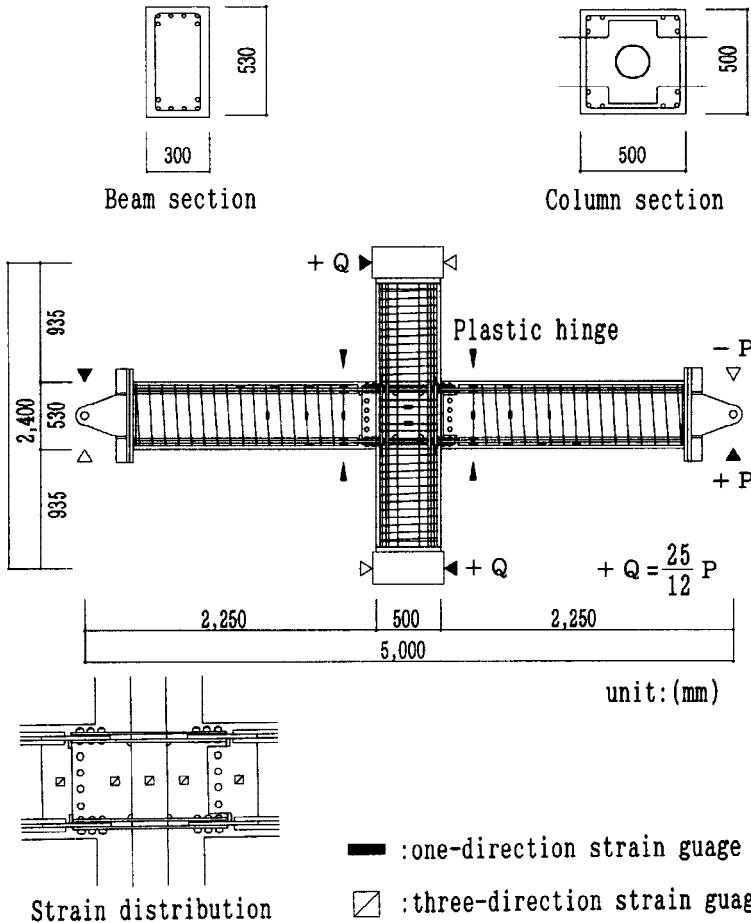


Fig. 2 Shape of test specimens and distribution of strain gauge

Table 2 Mechanical properties of used material

(a) Concrete

Test Specimen	Material age 1)	Compressive strength 2)	Tensile strength 2)	Young's modulus 3)
No. 1 JSCB1	8	242	22.9	2.10
No. 2 JDCB1	15	250	21.8	2.18
No. 3 JDCP1	19	249	18.5	2.20
No. 4 JDCP2	22	252	18.1	2.07
No. 5 JDTB1	27	265	21.8	2.22
No. 6 JDTP2	25	254	21.9	2.20
No. 7 J-CP3-1	11	271	23.7	2.66
No. 8 J-CP3-2	13	269	21.1	2.70
No. 9 RC-B	21	282	21.2	2.57
No. 10 RC-J	15	278	20.1	2.74

(b) Steel plate & reinforcing bar

Size	Grade	Yield stress 2)	Tensile strength 2)	Young's modulus 4)	Rupture Elongation 5)
No.1 ~ No.6					
PL4.5	SM490A	2710	4130	1.99	29.3
PL6	SM490A	3670	4930	1.95	27.1
PL9	SM490A	3620	5170	2.05	26.8
PL12	SM490A	4190	5440	2.17	24.6
PL16	SM490A	3840	5230	2.08	29.4
PL19	SM490A	4250	5360	2.11	24.6
PL25	SM490A	3660	5050	2.06	27.0
PL28	SM490A	3770	5230	2.05	31.3
165.2 φ x 4.5	STK400	3420	4250	2.05	36.3
D6	SD295A	3990	5330	1.80	22.1
D16	SD345	3910	5800	1.86	25.7
D19	SD345	3740	5730	1.85	23.5
D22	SD345	3950	6000	1.84	23.2
D25	SD345	3790	5650	1.91	25.8
U6.4	Deformed PC	13800	14900	1.94	8.2
No.7 ~ No.10					
PL9	SM490A	3750	5520	2.02	25.7
PL28	SM490A	3220	5230	1.97	30.2
165.2 φ x 7.1	STK400	4010	4870	2.02	35.3
216.3 φ x 5.8	STK400	3680	4510	1.84	32.9
D6	SD295A	4350	5780	1.92	29.2
D19	SD345	3800	5770	1.91	23.9
D25	SD345	3930	5810	1.94	23.8
D29	SD345	3750	5730	1.94	24.2
U6.4	Deformed PC	14040	15190	1.99	10.5

Unit : 1)Days, 2)kgf/cm<sup>2</sup>, 3) X 10<sup>5</sup> kgf/cm<sup>2</sup>, 4) X 10<sup>4</sup> kgf/cm<sup>2</sup>, 5)%

**Failure mode forecast**

The forecast of the maximum strength of each test specimen was found based on (1) to (5) from among standard formulae used in Japan.

**(A) Beam bending strength**

$$M_y = 0.9at \cdot \sigma_y \cdot d \dots \dots \dots (1)$$

**(B) Beam and Column shearing strength**

$$M_y = 0.8at \cdot \sigma_y \cdot D + 0.5 N \cdot D \{1 - N / (b \cdot D \cdot \sigma_B)\} \dots \dots \dots (2)$$

**(C) Column bending strength**

$$Q_{su} = 0.092 k_u \cdot k_p (180 + \sigma_B) / (a/d + 0.12) + 2.7\sqrt{pw \cdot w \cdot \sigma_y} \dots \dots \dots (3)$$

**(D) Joints shearing strength**

$$JMu = cVe (JFs \cdot J \delta + pw \cdot w \cdot \sigma_y) + 1.2sV \cdot s \cdot \sigma_y / \sqrt{3} \dots \dots \dots (4)$$

$$JMu = cVe (JFs \cdot J \delta + pw \cdot w \cdot \sigma_y) + 1.2sV \cdot s \cdot \sigma_y / \sqrt{3} + 1.2sV' \cdot s \cdot \sigma_y' / \sqrt{3} \dots \dots \dots (5)$$

$$Vju = \kappa \cdot \sigma_B \cdot b_j \cdot D \dots \dots \dots (6)$$

- My: Bending yield moment
- Qsu: Shearing strength
- JMu: Shearing strength panel moment
- Vju: Shearing strength affected on joint
- a: Shear span
- at: Sectional area of tension reinforcement
- b: Column width
- bj: Effective width of joint
- d: Effective depth
- D: Column depth
- JFs: Shearing strength of concrete
- ku, kp: Correction modulus of section
- N: Axial load
- cVe: effective volume of joint
- sV: effective volume of tube column
- sV': effective volume of web
- J δ : 3(crossing), 2(T shaped)
- κ : 0.30(crossing), 0.18(T shaped)
- σ\_y: Yield stress of main reinforcement
- σ\_y': Yield stress of tube column
- s σ\_y: Yield stress of web
- σ\_B: Compressive strength of concrete
- pw · w · σ\_y: Ratio of shear reinforcing bar

Table 3 shows the results of the above calculations. The forecast failure modes are determined from these formulae and presented on Table 1, but for this new structural system, No. 1, No. 2 and No. 5 were planned as bending yield type, No. 3 was planned as shearing failure type after beam bending yielding, and No. 4 and No. 6 were planned as joint shearing failure type. The calculation of these joint shear strengths was based on formula (4) and (5), and three cases were considered: the effect of the concrete, tube column, and web plates of joints; the joint shear resistance elements shown in Fig. 3. In the conventional reinforced concrete structure case, No. 9 was planned as a beam bending yield type in order to compare it with No. 2. And No. 10 was planned as joint shearing failure type.

Table 3 Calculated results

Test specimen	Beam		Column		Joint shearing strength		
	Bending Q1 (tonf)	Shearing Q2 (tonf)	Bending Q3 (tonf)	shearing Q2 (tonf)	Fig.3(a) Mju4 (t.m)	Fig.3(b) Mju5 (t.m)	RC type Vju6 (tonf)
NO. 1 JSCB1	14.7	42.0	45.7	38.2	72.1	79.9	
NO. 2 JDCB1	28.6	51.2	53.5	47.2	67.7	75.2	
NO. 3 JDCP1	41.9	73.2	65.1	59.9	65.2	78.1	
NO. 4 JDCP2	46.0	81.7	75.3	70.5	62.4	79.9	
NO. 5 JDTB1	14.3	25.8	53.8	47.9	51.3	55.0	
NO. 6 JDTP2	23.0	41.0	65.3	60.1	47.8	56.6	
NO. 7 J-CP3-1	58.9	83.9	77.5	75.5	72.0	89.9	
NO. 8 J-CP3-2	58.9	83.8	77.5	75.4	71.8	85.2	
NO. 9 RC-B	29.8	50.9	45.3	50.7			169.2
NO.10 RC-J	46.4	67.1	69.4	80.1			166.8

Q:Storey shearing force, Mju:Panel moment, Vju:Shearing force affected on joint

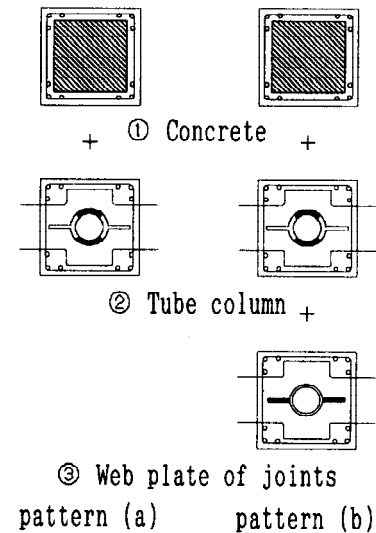


Fig.3 Joint shear resistance elements

**Testing method** Figure 4 shows the loading apparatus, Fig.5 shows the loading schedule, and Fig.6 shows the relationship of the deformation gauge point with the beam end angle. The loading was negative-positive alternating loading of beam input done with a manual hydraulic jack at the beam end. The column axial force was applied as a fixed axial force (Cruciform-type 0.2bDFc, T-shaped 0.1 bDFc) with a erectlic oil jack through pin-bearing to the column crown.

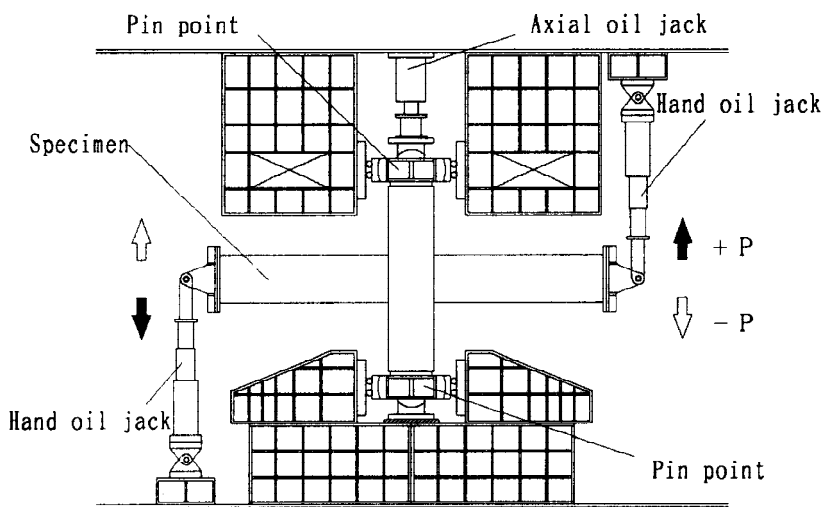


Fig.4 Loading apparatus

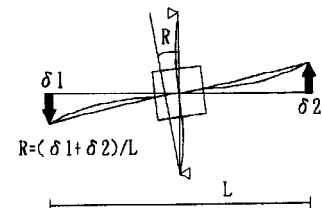


Fig.6 Relation of the deformation gauge point with the beam end angle

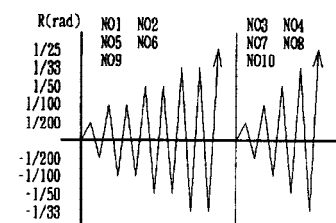


Fig.5 Loading schedule

**Test results**

**Failure process and failure mode** Figure 7 shows the ultimate failure state of each of the specimens. Observations of the state of cracking revealed that for all specimens, bending cracking appeared first near the hypothetical location of the yield hinge of the beam, followed by shearing cracking of the joint, and finally by bending cracking of the column. Bending cracking of the beam near the hinge in the beam bending yield types, Nos. 1, 2, 5, and 6, expanded as the load increased to become conspicuous bending yield type. Buckling of the main reinforcement in the beam was observed at the final cycle (R = 1/25rad.) in cases No. 1 and No 2. At that time, absolutely no damage was observed in the welded anchors of the reinforcement bars and the flange plates, confirming that sufficient anchor capacity was maintained, even under extremely large deformation.

In cases No. 3 and No. 4, bending yield of the beam was confirmed, but bending cracking of the beam did not advance, and at the final failure stage, shear cracks in the joint were widely expanded and cleaving cracks were observed along the main reinforcement bars of the columns within the joints, a state which can be defined as joint failure. Turning to the conventional reinforced concrete types No. 9 and No. 10, in the case of the beam bending yield type No. 9, after bending cracks appeared in the beam, cracking of the joint expanded as the load increased, and from the point when the joint translation angle  $R$  had almost reached  $1/50\text{rad.}$ , peeling of the concrete was observed at the joint, and when  $R = 1/20\text{rad.}$ , conspicuous joint failure occurred. In the case of No. 10, a joint failure type, from approximately  $R = 1/50\text{rad.}$ , considerable joint shearing cracking was noted, and repetition caused severe damage near the middle of the joint, reducing the strength.

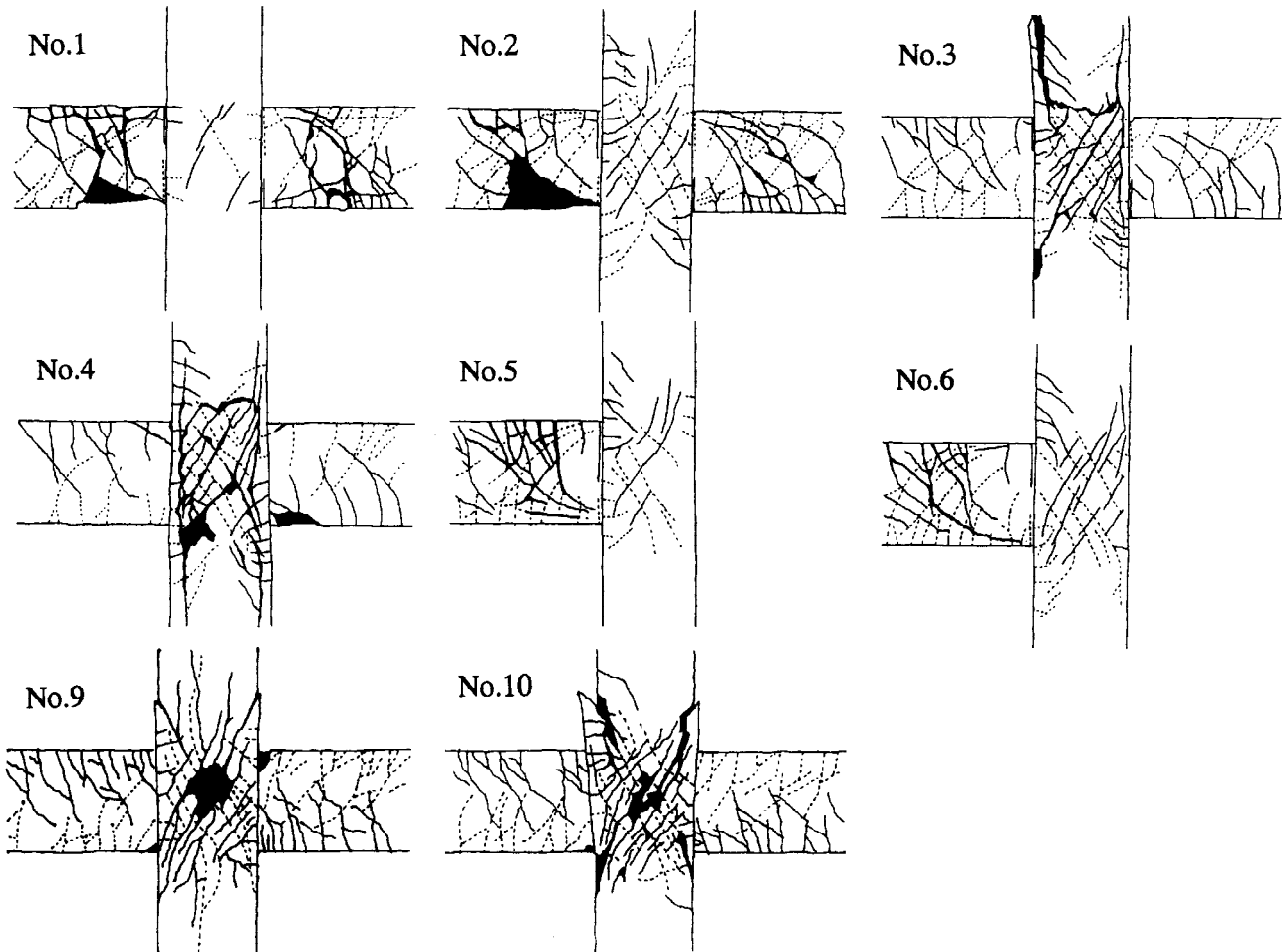


Fig.7 Ultimate failure state of each specimens

Hysteresis characteristics Figure 8 shows the relationship of the storey shearing force ( $Q$ ) with the joint translation angle ( $R$ ). The ordinate represents the shearing force (tonf) and the abscissa represents the joint translation angle (rad). In the beam bending yield types Nos. 1, 2, 5, and 6, the strength gradually increased after bending yielding, and in the No. 2 case, the strength was reduced by buckling of the main reinforcement, but up to the final cycle ( $R = 1/25\text{rad.}$ ), it displayed an extremely tough spindle-shaped loop shape. Repetitions at the same angle of deformation did not lower the strength, and its shape exceeded the previous cycle as is seen with steel frame structures. These are believed to be consequences of the small amount of sliding in this case, itself a result of the fact that there is a steel frame inside the joint and that the hinge is formed in the toe of the weld nearest to the center of the beam. In the case of specimen Nos. 3 and 4, up to the point where the joint translation angle  $R$  was close to  $1/60\text{rad.}$ , a stable loop form without any decline in the strength was observed, and when the maximum strength was achieved and  $R = 1/50\text{rad.}$ , the strength dropped, and the decline in the strength when it was  $1/25\text{rad.}$ , was 0.88 and 0.84 of the maximum strength for No. 3 and No. 4 respectively.

In the case of Nos. 2, 3, and 4, the steel tube inside the joints yields, and is an effective shear resistance element of the joint. In the case of Nos. 9 and 10, during repetitions from near a joint translation angle  $R = 1/100\text{rad.}$ , the strength declined against the previous cycle load, and when  $R = 1/60\text{rad.}$ , the strength dropped sharply to 0.80 against the previous load, slippage occurred, and the loop shape became a reversed S-shape. Regarding No. 5 and No. 6, the T-shaped specimens, in the case of both specimens, bending yielding was followed by a gentle climb in the strength, the strength did not decline till the final cycle, and stable hysteresis properties were obtained without any loss of strength caused by repetitions of the same cycle.

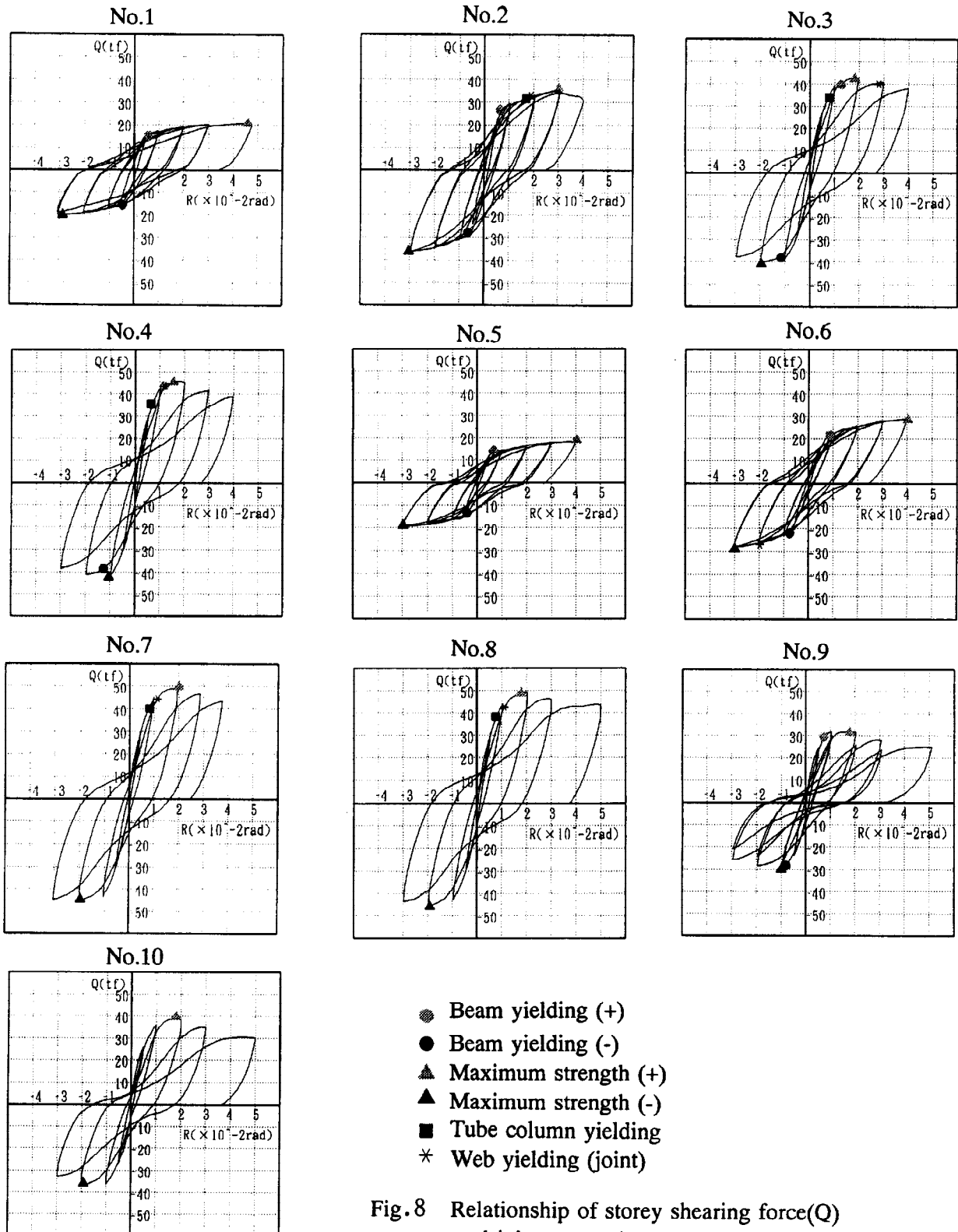


Fig. 8 Relationship of storey shearing force(Q) and joint translation angle(R)

Test values and calculated values Table 4 shows the storey shearing force (Q), the joint translation angle (R), and the failure mode at bending yield time and at maximum strength time obtained from the test results. This table also compares the test results with the calculated results. The bending yield of the beam was assessed at the point that the strain of the main reinforcement bars of the beam at the hypothetical yield hinge location reached the yield strain and the stiffness had declined conspicuously. This bending yield of the beam was confirmed for all specimens, but in cases No. 3 and No. 4, the joints were severely damaged, and appeared to have undergone joint failure. The bending strength of the beam was within a range between 0.79 and 1.07 times the values computed based on formula (1), a simplified reinforced concrete formula.

Table 4 Experimental results

Test specimen	Beam bending yielding time			Maximum strength time		Joint shear stress affected on concrete at maximum load $\tau$ (kgf/cm <sup>2</sup> )				Failure mode of experiment
	Q (tonf)	R (rad.)	Exp. Cal. <sup>1)</sup>	Q (tonf)	R (rad.)	Fig.3 (a)		Fig.3 (b)		
						$\tau$	$\tau/\sigma_B$	$\tau$	$\tau/\sigma_B$	
No. 1 JSCB1	15.8	1/166	1.07	20.7	1/22	29.4	0.12	21.4	0.09	B
No. 2 JDCB1	27.0	1/154	0.94	36.1	1/33	65.5	0.26	57.7	0.23	B
No. 3 JDCP1	40.2	1/81	0.96	42.9	1/56	82.6	0.33	68.6	0.28	J
No. 4 JDCP2	43.5	1/83	0.95	45.3	1/62	91.5	0.36	72.2	0.29	J
No. 5 JDTB1	13.9	1/157	0.97	18.8	1/25	28.6	0.11	24.7	0.09	B
No. 6 JDTP2	21.5	1/118	0.93	28.6	1/25	53.3	0.21	43.7	0.17	B
No. 7 J-CP3-1	—	—	—	49.3	1/51	92.9	0.34	72.7	0.27	J
No. 8 J-CP3-2	—	—	—	48.8	1/56	91.8	0.34	76.8	0.29	J
No. 9 RC-B	29.4	1/136	0.99	31.3	1/56	62.4	0.22			B-J
No.10 RC-J	—	—	—	39.4	1/55	86.3	0.31			J

Q:Storey shearing force, R:Joint translation angle

Strain properties Figure 9 shows the strain distribution near the joints in No. 2 and No. 9 as an example of a comparison of the new structural system with the conventional reinforced concrete structural system. It shows that in the No. 2 case, the maximum value of the strain was obtained at the hypothetical location of the yield hinge, and that inside the joint, the yield strain was not achieved. This indicates that the yield hinge formed at the hypothetical yield hinge location, and that its adhesive properties were good. And in the case of No. 9, near 1/800rad at the initial loading stage, the strain in the critical section was great, and beginning at about 1/100rad, where the tension reinforcement bars achieved yield strain, the strain in the compression side reinforcement bars was transformed into tensile strain, and the adhesive force of the main reinforcement in the beams declined.

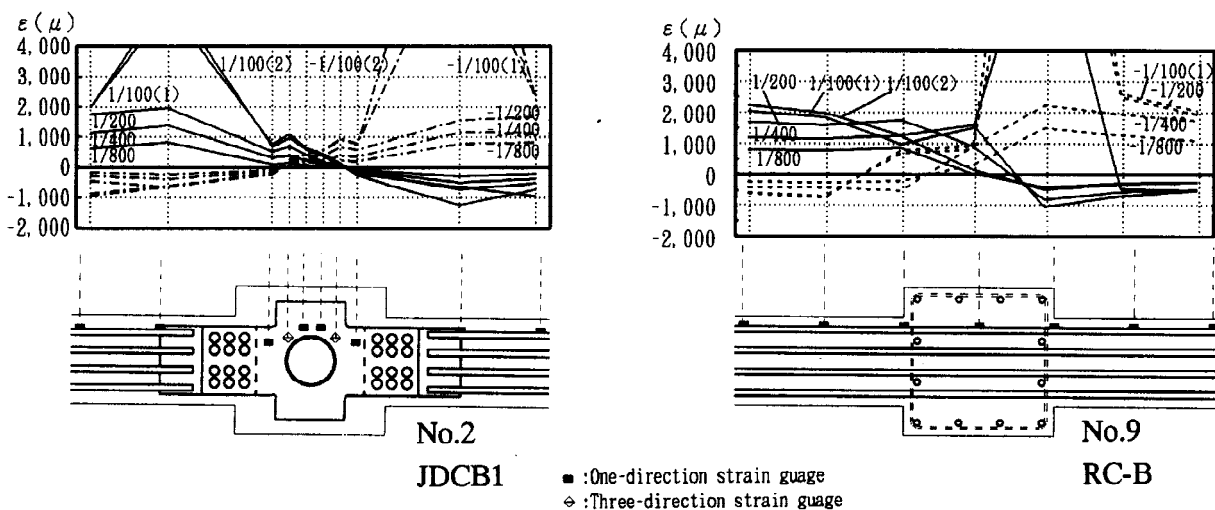


Fig.9 The strain distribution

**Joint shearing deformation Angle** Figure 10 shows the storey shearing force (Q) - shear deformation angle ( $\gamma$ ) curves for Nos. 2, 4, and 9. The shear deformation was found as shown in the typical diagram shown in Fig.10-(a). This supports the view that with this new structural system, there is little deformation of the joints up to the ultimate stage as shown in Fig.10-(b), and bending yield of the beam is formed. The conventional reinforced concrete structural system specimen No. 9 supports the conclusion that repetitive loading is accompanied by an increase in the shear deformation angle and damage to the joint causes failure.

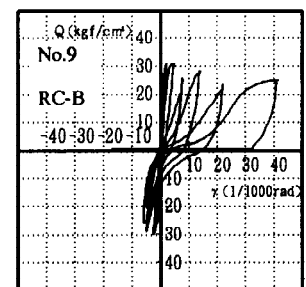
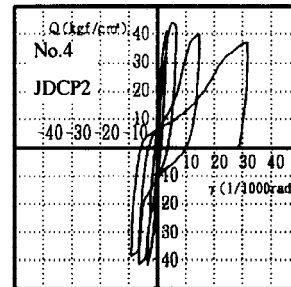
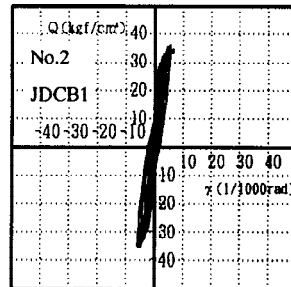
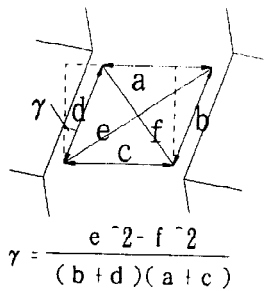


Fig.10-(a) Typical diagram      Fig.10-(b) Storey shearing force (Q)-shear deformation angle ( $\gamma$ )

**Study of the Results** The following is a comparison of the strength of the joints and failure condition of the new structural system and the conventional reinforced concrete structural system.

- 1) **Failure Properties** A comparison of the beam yield types, No. 2 and No. 9, reveals that in contrast to No. 2 where the damage was concentrated at the hypothetical hinge location and it was clearly a beam failure, in the No. 9 specimen, regardless of damage to the beam, joint failure was severe, and its performance was determined by the properties of the joints.
- 2) **Deformation Properties** The load - deformation curve for No. 2 is spindle-shaped loop until large deformation occurs, and displays extremely tough behavior, but when 1/100rad. is exceeded in the conventional reinforced concrete specimen, slippage of the main reinforcement bars and damage to the joints forms a reverse S-shaped loop, and at the stage where the value exceeds 1/60rad., the repetitive loading reduces the strength substantially.

## CONCLUSIONS

- 1) The joints are extremely tough, and it is possible to cause the steel reinforcement to yield reliably at the hypothetical hinge location in the beam material to guarantee beam flexure.
- 2) The method of welding the main reinforcement steel of the beams can be used as an anchoring method that prevents damage, even after the buckling of the steel reinforcement and achievement of the ultimate state.
- 3) The new structural system specimens absorb more energy than the specimens of the conventional reinforced concrete structures, providing superior earthquake resistance.

## REFERENCES

- Architectural Institute of Japan (1973). Design Standard for Steel Structures.
- Architectural Institute of Japan (1991). Standard for Structural Calculation of Reinforced Concrete Structures.
- Architectural Institute of Japan (1990). Design Guidelines for Earthquake Resistant Reinforced Concrete Buildings Based on Ultimate Strength Concept. (in Japanese)
- Architectural Institute of Japan (1987). Standard for Structural Calculation of Steel Reinforced Concrete Structures.